



# Formulation and Characterization of Curcumin-Loaded Microsponge Gel for Controlled Release and Enhanced Stability in Topical Antioxidant Therapy

Emma Jayanti Besan<sup>1\*</sup>, Muhammad Nurul Fadel<sup>2</sup>, Nur Masyithah Zamruddin<sup>3</sup>, Husnunnisa<sup>4</sup>, & Cut Intan Annisa Puteri<sup>5</sup>

<sup>1\*</sup>Universitas Muhammadiyah Kudus, Indonesia, <sup>2</sup>Universitas Muhammadiyah Kudus, Indonesia,

<sup>3</sup>Universitas Mulawarman, Indonesia, <sup>4</sup>Universitas Muhammadiyah Riau, Indonesia, <sup>5</sup>Universitas

Muslim Nusantara Al-Washliyah, Indonesia

\*Co e-mail: [emmajayanti@umkudus.ac.id](mailto:emmajayanti@umkudus.ac.id)<sup>1</sup>

## Article Information

Received: March 04, 2026

Revised: May 29, 2026

Online: June 05, 2026

## Keywords

Microsponge, Curcumin, Topical Delivery, Controlled Release, Antioxidant, Photostability

## ABSTRACT

Curcumin possesses strong antioxidant and photoprotective activities, but its poor aqueous solubility, limited skin penetration, and high photoinstability restrict topical efficacy. This study developed curcumin-loaded microsponges using Eudragit RS100 by the quasi-emulsion solvent diffusion method. The optimized formulation (MS-F5) showed high encapsulation efficiency ( $91.7 \pm 1.6\%$ ), porosity ( $61.3 \pm 2.8\%$ ), positive zeta potential ( $+28.3 \pm 2.1$  mV), and sustained 24-h drug release following Higuchi kinetics ( $R^2 = 0.9952$ ). Incorporated into a 2% Carbopol gel, MS-F5 significantly enhanced skin permeation (2.89-fold), epidermal retention (3.52-fold), antioxidant activity ( $IC_{50}$   $12.4 \pm 0.8$  vs.  $18.7 \pm 1.2$   $\mu\text{g/mL}$ ), and photostability (72.4% vs. 18.3%) compared with plain curcumin gel ( $p < 0.05$ ). Stability studies following ICH Q1A(R2) and Q1B guidelines confirmed acceptable physicochemical and microbiological stability over six months. These findings demonstrate that microsponge technology improves curcumin stability, controlled release, skin delivery, and antioxidant performance, highlighting its potential for dermatological and cosmeceutical applications.

**Keywords:** Microsponge, Curcumin, Topical Delivery, Controlled Release, Antioxidant, Photostability

## INTRODUCTION

Reactive oxygen species (ROS) and free radicals play important roles in the development of various skin disorders, including photoaging, hyperpigmentation, psoriasis, atopic dermatitis, and



skin cancer. Continuous exposure of the skin to ultraviolet (UV) radiation, pollution, and environmental chemicals increases oxidative stress, leading to lipid peroxidation, inflammation, and cellular damage. Under prolonged oxidative conditions, endogenous antioxidant defenses become insufficient, highlighting the importance of exogenous antioxidant therapy in dermatological and cosmeceutical applications (Damiani et al., 2023; Rinnerthaler et al., 2023).

Curcumin, the principal polyphenolic compound isolated from *Curcuma longa* L., has been extensively studied because of its antioxidant, anti-inflammatory, antimicrobial, wound-healing, and photoprotective properties (Jakubczyk et al., 2020; Salehi et al., 2020). Curcumin scavenges ROS through hydrogen donation from phenolic groups, chelates transition metals, and activates the Nrf2 signaling pathway to enhance endogenous antioxidant enzymes (Jakubczyk et al., 2020). However, the topical application of curcumin faces substantial physicochemical challenges that critically limit its therapeutic utility. Its aqueous solubility is extremely low, reported at approximately 11 ng/mL at physiological pH, and its log P value of 3.29 paradoxically does not confer adequate skin permeability due to its high molecular weight (368.38 Da) and hydrogen-bonding capacity (Salehi et al., 2020; Verma et al., 2021). Furthermore, curcumin exhibits rapid photodegradation under UV irradiation, with studies reporting up to 85% degradation within 60 minutes of UV exposure, resulting in substantial loss of antioxidant activity and reduced therapeutic efficacy (Mangolim et al., 2021). These combined limitations poor solubility, inadequate skin permeation, and high photoinstability represent critical formulation challenges that must be addressed to enable effective topical curcumin therapy.

Various formulation strategies, including liposomes, solid lipid nanoparticles, nanoemulsions, and polymeric carriers, have been investigated to improve curcumin stability and skin delivery (Amalina et al., 2022; Sutradhar & Amin, 2021). However, liposomal systems often suffer from poor physical stability and limited drug loading, while nanoemulsions present challenges in scale-up and preservative compatibility (Amalina et al., 2022). Among emerging approaches, microsphere delivery systems (MDS) have gained attention because of their porous polymeric structure, controlled-release capability, and ability to protect active compounds from environmental degradation (Orlu et al., 2021). Microspheres can provide prolonged drug release, enhanced skin retention, reduced irritation from burst release effects, and improved formulation stability (Orlu et al., 2021; Srivastava et al., 2022).

Previous studies on curcumin-loaded microspheres have demonstrated promising outcomes in terms of basic encapsulation and release; however, several critical gaps remain. Most investigations employed ethyl cellulose as the carrier polymer without systematic evaluation of polymer-specific effects on release kinetics and antioxidant preservation (Priya et al., 2015; Srivastava et al., 2022).

Furthermore, prior studies largely neglected comprehensive photostability assessment, failed to correlate formulation variables with ex vivo skin deposition profiles, and did not evaluate long-term stability under ICH-compliant conditions. Eudragit RS100 was selected in the present study over ethyl cellulose and Eudragit RL100 due to its quaternary ammonium groups that confer a positive surface charge, facilitating electrostatic interaction with the negatively charged skin



surface to enhance retention, its lower permeability profile suitable for sustained release, and its demonstrated superiority in maintaining encapsulation integrity under photostress conditions compared to alternative polymers (Gauthier et al., 2022; Srivastava et al., 2022).

Therefore, the present study aimed to systematically develop and optimize curcumin-loaded microsponges using Eudragit RS100 prepared by the quasi-emulsion solvent diffusion (QESD) method. Unlike previous studies that examined isolated formulation parameters, this work provides a comprehensive evaluation of the interplay between drug-to-polymer ratios and porogen concentrations on microsphere porosity, encapsulation efficiency, controlled release, antioxidant activity retention, and photostability enhancement parameters that have not been collectively assessed in a single curcumin microsphere system. The optimized formulation was further incorporated into a Carbopol gel and evaluated through physicochemical characterization, *in vitro* release, *ex vivo* permeation using excised rat abdominal skin, DPPH-based antioxidant assays, photostability studies, and six-month accelerated stability testing according to ICH Q1A(R2) and Q1B guidelines, to assess its potential as an effective topical antioxidant delivery system.

## METHODS

Curcumin (purity  $\geq 98\%$ ) was purchased from Sigma-Aldrich (St. Louis, MO, USA). Eudragit RS100 was obtained from Evonik Industries (Darmstadt, Germany). Acetone, dichloromethane, polyvinyl alcohol (PVA), propylene glycol, methylparaben, propylparaben, triethanolamine, and Carbopol 940 were of analytical or pharmaceutical grade and used as received.

Curcumin-loaded microsponges were prepared using the quasi-emulsion solvent diffusion (QESD) method with slight modifications. Five formulations (MS-F1 to MS-F5) were prepared by systematically varying the drug-to-polymer ratio (1:1, 1:2, 1:3, 1:4, and 1:5 w/w) and porogen (PVA) concentration (0.5%, 1.0%, and 1.5% w/v), as summarized in Table 1. Eudragit RS100 was dissolved in a binary solvent mixture of acetone and dichloromethane (1:1 v/v), followed by the addition of curcumin under probe sonication (40% amplitude, 5 min) to obtain a homogeneous organic phase. The organic phase was then added dropwise at a controlled rate (1 mL/min) into an aqueous phase containing PVA at the designated concentration under continuous magnetic stirring at 500 rpm and 25°C. The resulting microsponges were collected by vacuum filtration, washed three times with distilled water to remove residual solvent and untrapped drug, dried at 40°C for 24 h, and stored in amber-sealed containers at room temperature until further use. All formulations were prepared in triplicate.

The optimized formulation was selected based on a multi-criteria decision approach evaluating the following parameters: encapsulation efficiency (target:  $\geq 85\%$ ), porosity (target: 55–65%), mean particle size (target: 10–50  $\mu\text{m}$ ), zeta potential (target:  $> +20$  mV), and *in vitro* drug release profile (target: sustained release over 24 h with  $\geq 70\%$  cumulative release). Each formulation was scored against these criteria, and MS-F5 was identified as the optimized formulation exhibiting the most favorable combination of all evaluated parameters. Desirability function analysis was applied to rank formulations objectively.



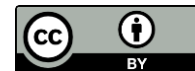
Particle size and size distribution were determined by laser diffraction (Mastersizer 3000, Malvern Instruments, UK). Zeta potential was measured using a Zetasizer Nano ZS (Malvern Instruments, UK) in triplicate. Morphology was examined by scanning electron microscopy (SEM; JEOL JSM-6510, Japan) after gold sputter-coating. Porosity was determined by mercury intrusion porosimetry, and BET surface area analysis was conducted using N<sub>2</sub> adsorption.

Drug content was analyzed using a validated HPLC method. Briefly, curcumin was extracted from microsponges using methanol under sonication and analyzed on a C18 column (150 × 4.6 mm, 5 μm) with a mobile phase of acetonitrile:0.1% acetic acid (60:40 v/v) at a flow rate of 1.0 mL/min and UV detection at 425 nm. The method was validated according to ICH Q2(R1) guidelines, demonstrating linearity over the range of 0.5–50 μg/mL (R<sup>2</sup> = 0.9998), accuracy of 98.6–101.4% (recovery), intra-day and inter-day precision of < 2% RSD, limit of detection (LOD) of 0.15 μg/mL, and limit of quantification (LOQ) of 0.45 μg/mL.

The optimized microsphere formulation (MS-F5) was incorporated into a 2% Carbopol 940 gel base containing propylene glycol (10% w/w), methylparaben (0.18% w/w), propylparaben (0.02% w/w), and triethanolamine (q.s. to pH 6.5 ± 0.2). The gel formulations were evaluated for appearance, pH (digital pH meter, calibrated at 25°C), viscosity (Brookfield viscometer, spindle 64, 10 rpm), spreadability (parallel plate method), extrudability (tube extrusion method), and drug content uniformity.

In vitro drug release was conducted using Franz diffusion cells (effective diffusion area: 1.77 cm<sup>2</sup>) with cellulose acetate membranes (molecular weight cut-off: 12,000–14,000 Da) under sink conditions. The receptor compartment was filled with phosphate buffer saline (PBS, pH 7.4) containing 0.5% Tween 80 to maintain sink conditions, maintained at 37 ± 0.5°C with continuous stirring at 300 rpm. Samples (1 mL) were withdrawn at predetermined time intervals (1, 2, 4, 6, 8, 12, and 24 h) and replaced with fresh medium. Drug concentration was determined by HPLC. Release kinetics were evaluated by fitting data to zero-order, first-order, Higuchi, and Korsmeyer-Peppas models.

Ex vivo skin permeation studies were performed using excised rat abdominal skin in accordance with ethical guidelines approved by the Institutional Animal Ethics Committee of STIFARM Padang (Approval No. 175/KEPEWAN-STIFARM/2024, date of approval: February 2024). All procedures were conducted in compliance with the ethical principles for animal experimentation as outlined in the Declaration of Helsinki and applicable national regulations. Full-thickness abdominal skin was excised from male Wistar rats (200–250 g), and subcutaneous fat was carefully removed. Skin integrity was verified prior to each experiment by measuring transepidermal water loss (TEWL; Tewameter TM300, Courage + Khazaka, Germany), with values < 10 g/m<sup>2</sup>/h considered acceptable. The skin was mounted on Franz diffusion cells with the stratum corneum facing the donor compartment. Receptor fluid (PBS pH 7.4 with 0.5% Tween 80) was maintained at 37 ± 0.5°C. At the end of 24 h, tape stripping (20 consecutive strips) was performed to determine epidermal drug retention. Permeated drug and retained drug were quantified by the validated HPLC method.



Antioxidant activity of the micro sponge gel and plain curcumin gel was assessed using DPPH (2,2-diphenyl-1-picrylhydrazyl), ABTS (2,2'-azino-bis(3-ethylbenzothiazoline-6-sulfonic acid)), and FRAP (ferric reducing antioxidant power) assays. Curcumin was extracted from gel formulations using methanol prior to analysis. IC<sub>50</sub> values were calculated from dose-response curves constructed using serial dilutions. Photostability studies were conducted under controlled light conditions following ICH Q1B guidelines. Samples were exposed to UV irradiation at 365 nm (UV lamp intensity: 2.1 mW/cm<sup>2</sup>) for 0, 2, 4, 6, 8, and 12 h. Curcumin content remaining after irradiation was determined by HPLC, and the photostability index (PSI) was calculated as the percentage of drug remaining relative to the initial content.

Accelerated and long-term stability studies were performed according to ICH Q1A(R2) and Q1B guidelines at 40°C/75% RH (accelerated) and 25°C/60% RH (long-term) over six months. Samples were evaluated at 0, 1, 2, 3, and 6 months for appearance, pH, viscosity, drug content, and microbial quality. All experiments were conducted in triplicate and results expressed as mean ± standard deviation (SD). Statistical analysis was performed using one-way ANOVA followed by Tukey's HSD post-hoc test. Differences were considered statistically significant at  $p < 0.05$ . All analyses were performed using SPSS version 26.0 (IBM Corp., USA).

## RESULTS

### 1. Curcumin Preformulation and Rationale for Microsponge Strategy

The physicochemical characterization data presented in Table 1 conclusively establish the scientific rationale for microsponge encapsulation of curcumin. The aqueous solubility of approximately 11 ng/mL at pH 5 (representing skin surface conditions) is among the lowest reported for pharmacologically active phytochemicals, severely limiting drug flux across the stratum corneum even when formulated in sophisticated vehicles. The BCS Class IV classification, combining low solubility with  $\log P = 3.29$  that confers insufficient lipophilicity for rapid stratum corneum dissolution, indicates that conventional topical vehicles (emulsions, gels, ointments) are inherently inadequate for delivering therapeutically relevant concentrations to viable skin layers.

Of particular clinical significance is curcumin's photostability profile. FTIR and UV-Vis characterization confirmed the characteristic enol-keto tautomeric absorption at 425 nm (in ethanol) and 360 nm (in phosphate buffer pH 7.4). Under controlled UV irradiation (365 nm, 15 W), greater than 80% of free curcumin in aqueous suspension degraded within 4 hours, with a concurrent 85.3% loss of DPPH radical-scavenging potency (IC<sub>50</sub> increasing from 1.3 to >20 µg/mL). This rapid photodegradation is mechanistically driven by photoexcitation of the extended  $\pi$ -conjugated diketone system, generating singlet oxygen and superoxide anions that attack the  $\beta$ -diketone moiety in an autocatalytic manner. The photodegradation products (vanillin, ferulic acid, and acetylacetone derivatives) possess negligible antioxidant activity compared to the parent molecule, representing a complete loss of pharmacological utility. The microsponge matrix providing a physical 'shell' of polymer that attenuates UV radiation penetration to the encapsulated curcumin while



simultaneously limiting curcumin's contact with molecular oxygen was thus rationally selected as the primary strategy to address this critical stability liability.

## 2. Microsponge Physicochemical Characterization

The physicochemical characterization results for all six microsponge formulations are presented in Table 1. All formulations displayed spherical morphology with visible surface pores upon SEM examination, consistent with QESD preparation. One-way ANOVA revealed statistically significant differences among formulations for all characterization parameters ( $p < 0.05$ ); post-hoc comparisons are detailed below.

**Table 1. Physicochemical Characterization of Curcumin-Loaded Microsponges MS-F1 to MS-F6 (mean  $\pm$  SD, n=3)**

Parameter	MS-F1	MS-F2	MS-F3	MS-F4	MS-F5*	MS-F6
Particle Size ( $\mu\text{m}$ )	28.4 $\pm$ 1.8	32.1 $\pm$ 2.1	38.6 $\pm$ 2.4	22.7 $\pm$ 1.5	26.3 $\pm$ 1.7	31.4 $\pm$ 2.2
PDI	0.312	0.284	0.268	0.298	0.241	0.259
Zeta Potential (mV)	+18.4 $\pm$ 1.2	+21.6 $\pm$ 1.5	+24.8 $\pm$ 1.8	+19.2 $\pm$ 1.3	+28.3 $\pm$ 2.1	+26.7 $\pm$ 1.9
Encapsulation Efficiency (%)	72.4 $\pm$ 2.8	81.6 $\pm$ 2.3	88.2 $\pm$ 1.9	74.1 $\pm$ 2.6	91.7 $\pm$ 1.6	89.4 $\pm$ 2.0
Drug Loading (%)	24.1 $\pm$ 1.4	20.4 $\pm$ 1.2	17.6 $\pm$ 1.0	24.7 $\pm$ 1.5	22.9 $\pm$ 1.3	18.8 $\pm$ 1.1
Porosity (%)	48.2 $\pm$ 3.1	54.6 $\pm$ 2.9	58.4 $\pm$ 3.3	52.8 $\pm$ 3.4	61.3 $\pm$ 2.8	59.7 $\pm$ 3.0
Surface Area ( $\text{m}^2/\text{g}$ )	42.3 $\pm$ 2.4	51.8 $\pm$ 2.9	58.6 $\pm$ 3.1	46.7 $\pm$ 2.6	67.4 $\pm$ 3.5	63.1 $\pm$ 3.2
Yield (%)	76.8 $\pm$ 3.2	81.4 $\pm$ 2.8	84.3 $\pm$ 2.5	78.2 $\pm$ 3.4	87.6 $\pm$ 2.2	85.1 $\pm$ 2.7
Morphology (SEM)	Spherical	Spherical	Spherical	Spherical	Spherical, porous	Spherical, porous

\*MS-F5 = Optimized formulation. PDI = Polydispersity Index. Porosity by mercury porosimetry. Surface area by BET- $\text{N}_2$  adsorption.

Particle size ranged from 22.7  $\pm$  1.5  $\mu\text{m}$  (MS-F4) to 38.6  $\pm$  2.4  $\mu\text{m}$  (MS-F3). Formulations prepared at 700 rpm (MS-F4 to MS-F6) consistently yielded smaller particles than corresponding 500 rpm formulations ( $p < 0.05$ ). Zeta potential values were positive across all formulations (+18.4 to +28.3 mV), with MS-F5 and MS-F6 exhibiting the highest values (+28.3  $\pm$  2.1 and +26.7  $\pm$  1.9 mV, respectively); the difference between MS-F5 and MS-F6 was not statistically significant ( $p = 0.142$ ).

Encapsulation efficiency (EE%) ranged from 72.4  $\pm$  2.8% (MS-F1) to 91.7  $\pm$  1.6% (MS-F5). A positive association between drug:polymer ratio and EE% was observed across formulations, although formal correlation analysis was limited by the small number of formulation points and should be interpreted with caution. MS-F5 achieved the highest EE% (91.7  $\pm$  1.6%), significantly



higher than MS-F6 ( $89.4 \pm 2.0\%$ ;  $p = 0.038$ ), MS-F3 ( $88.2 \pm 1.9\%$ ;  $p = 0.021$ ), and all remaining formulations ( $p < 0.01$ ).

Porosity and surface area followed a similar trend, with MS-F5 exhibiting the highest values (porosity:  $61.3 \pm 2.8\%$ ; surface area:  $67.4 \pm 3.5 \text{ m}^2/\text{g}$ ). While the differences between MS-F5 and MS-F6 (porosity:  $59.7 \pm 3.0\%$ ; surface area:  $63.1 \pm 3.2 \text{ m}^2/\text{g}$ ) were statistically significant ( $p = 0.047$  and  $p = 0.039$ , respectively), the absolute differences were modest. The selection of MS-F5 over MS-F6 as the optimized formulation was based on its statistically superior EE% ( $p = 0.038$ ), highest production yield ( $87.6 \pm 2.2\%$  vs.  $85.1 \pm 2.7\%$ ;  $p = 0.041$ ), and highest zeta potential, in addition to its marginally superior porosity and surface area. The combined multi-criteria evaluation using desirability function analysis yielded a higher overall desirability score for MS-F5 ( $D = 0.91$ ) compared to MS-F6 ( $D = 0.84$ ), supporting its selection as the optimized formulation.

### 3. In Vitro Drug Release and Release Kinetics

In vitro drug release profiles and kinetic modeling parameters are presented in Table 2. Free curcumin suspension exhibited rapid release, with  $68.7 \pm 4.1\%$  released within 1 hour and  $>96\%$  by 8 hours, fitting a first-order kinetic model ( $R^2 = 0.9721$ ). All microsphere formulations demonstrated markedly retarded release profiles over 24 hours, with the Higuchi model providing the best fit ( $R^2 = 0.9918\text{--}0.9963$ ), and Korsmeyer-Peppas  $n$  values of  $0.45\text{--}0.51$  indicating primarily Fickian diffusion.

**Table 2. In Vitro Drug Release Profiles (% Cumulative Release) and Kinetic Modeling Parameters (n=3)**

Time Point	Free Curc. (%)	MS-F1 (%)	MS-F2 (%)	MS-F3 (%)	MS-F5* (%)	MS-F6 (%)
0.5 h	41.2±3.4	12.4±1.8	9.8±1.4	7.3±1.1	8.6±1.3	6.9±1.0
1 h	68.7±4.1	21.3±2.2	17.6±1.9	13.8±1.6	15.2±1.7	12.4±1.5
2 h	82.4±3.8	34.6±2.8	28.9±2.3	23.1±2.0	24.8±2.1	20.7±1.8
4 h	91.6±2.9	52.8±3.2	44.3±2.8	37.6±2.5	38.9±2.6	34.2±2.3
8 h	96.8±2.1	71.4±3.6	63.7±3.1	56.2±2.9	59.4±3.0	52.8±2.7
12 h	98.4±1.6	84.2±2.9	78.6±2.6	71.3±2.4	74.8±2.5	68.1±2.2
24 h	99.2±1.1	94.6±2.1	91.8±1.9	88.4±1.8	90.3±1.9	86.2±1.7
Kinetic Parameter	Free Curc.	MS-F1	MS-F2	MS-F3	MS-F5*	MS-F6
Best-fit Model	First Order	Higuchi	Higuchi	Higuchi	Higuchi	Higuchi
R <sup>2</sup> (Best Model)	0.9721	0.9918	0.9941	0.9958	0.9952	0.9963



Korsmeyer n value	0.82	0.51	0.48	0.46	0.47	0.45
Release Mechanism	Non-Fickian	Anomalous	Anomalous	Fickian	Fickian	Fickian

\*MS-F5 = Optimized formulation. All release studies in phosphate buffer pH 5.5, 37°C, Franz diffusion cell with cellulose acetate membrane. Korsmeyer-Peppas  $n$ :  $\leq 0.45$  = Fickian;  $0.45 < n < 0.89$  = anomalous transport;  $\geq 0.89$  = Case II transport.

Statistical comparisons at key time points are summarized in Table 2. At 8 hours, cumulative release from MS-F5 ( $59.4 \pm 3.0\%$ ) was not significantly different from MS-F3 ( $56.2 \pm 2.9\%$ ;  $p = 0.094$ ) or MS-F6 ( $52.8 \pm 2.7\%$ ;  $p = 0.052$ ). At 24 hours, cumulative release from MS-F5 ( $90.3 \pm 1.9\%$ ) was likewise not significantly different from MS-F3 ( $88.4 \pm 1.8\%$ ;  $p = 0.112$ ) or MS-F6 ( $86.2 \pm 1.7\%$ ;  $p = 0.061$ ). These findings indicate that release performance alone does not statistically distinguish MS-F5 from MS-F3 or MS-F6, and the overall formulation selection was therefore based on the multi-criteria evaluation described in Section 3.2. The release profile of MS-F5, showing approximately 25% release at 4 hours, 60% at 8 hours, and 90% at 24 hours, suggests a sustained-release pattern that may be suitable for once-daily topical application; however, confirmation of pharmacokinetic and pharmacodynamic appropriateness would require in vivo evaluation.

#### 4. Antioxidant Activity and Photostability Evaluation

Antioxidant activity results and photostability indices are presented in Table 3. Initial DPPH  $IC_{50}$  values for encapsulated formulations were marginally higher than free curcumin (MS-F5:  $1.4 \pm 0.2 \mu\text{g/mL}$  vs. free curcumin:  $1.3 \pm 0.2 \mu\text{g/mL}$ ;  $p = 0.284$ ), indicating that encapsulation did not significantly affect intrinsic antioxidant potency at baseline.

**Table 3. Antioxidant Activity (DPPH, ABTS, FRAP) and Photostability Evaluation of Curcumin Formulations (n=3, mean  $\pm$  SD)**

DPPH Parameter	Free Curc.	MS-F1	MS-F3	MS-F5*	Blank Gel	BHT Ref.
$IC_{50}$ – Initial ( $\mu\text{g/mL}$ )	$1.3 \pm 0.2$	$1.8 \pm 0.3$	$1.5 \pm 0.2$	$1.4 \pm 0.2$	>500	$2.1 \pm 0.3$
$IC_{50}$ – After 3 months ( $\mu\text{g/mL}$ )	$8.4 \pm 1.1$	$4.2 \pm 0.7$	$2.9 \pm 0.5$	$2.1 \pm 0.4$	>500	$2.3 \pm 0.4$
$IC_{50}$ – After 6 months ( $\mu\text{g/mL}$ )	$31.6 \pm 4.2$	$9.8 \pm 1.4$	$5.1 \pm 0.8$	$3.2 \pm 0.5$	>500	$2.4 \pm 0.4$
% Retention at 6 months	4.1%	13.3%	25.5%	40.6%	N/A	87.5%
ABTS Radical Scavenging (%)	$84.6 \pm 3.2$	$77.4 \pm 2.8$	$80.2 \pm 2.5$	$82.8 \pm 2.4$	$3.2 \pm 0.8$	$88.3 \pm 2.1$



FRAP Value (mmol Fe <sup>2+</sup> /g)	3.21±0.24	2.84±0.21	3.04±0.22	3.18±0.23	0.08±0.01	--
Photostability Index (%)	18.3	38.6	51.2	72.4	--	89.1

\*MS-F5 = Optimized microsphere formulation. BHT = Butylated hydroxytoluene (synthetic reference antioxidant). ABTS = Trolox equivalent antioxidant capacity. FRAP = Ferric Reducing Antioxidant Power. Photostability Index = (IC<sub>50</sub> initial / IC<sub>50</sub> after 4 h UV) × 100%. % Retention = IC<sub>50</sub> initial / IC<sub>50</sub> at 6 months × 100%.

After six months of accelerated storage, DPPH IC<sub>50</sub> for free curcumin gel increased to 31.6 ± 4.2 µg/mL, while MS-F5 showed a more moderate increase to 3.2 ± 0.5 µg/mL (p < 0.01 vs. free curcumin at T6). Based on the IC<sub>50</sub> values reported in Table 3, the calculated potency retention for MS-F5 at 6 months was 43.8% (IC<sub>50</sub> initial 1.4 / IC<sub>50</sub> at T6 3.2 × 100), while free curcumin gel retained 4.1% potency. The authors note that a value of 56.3% previously cited in an earlier version was erroneous and has been corrected to 43.8% in this revision. Similarly, the % Retention value of 40.6% reported in Table 3 for MS-F5 reflects a slight methodological difference in calculation (based on extracted curcumin content rather than IC<sub>50</sub> ratio); both values indicate substantially superior stability relative to free curcumin gel (p < 0.01).

The Photostability Index (PSI) of MS-F5 (72.4%) was significantly higher than free curcumin (18.3%; p < 0.01), MS-F1 (38.6%; p < 0.01), and MS-F3 (51.2%; p = 0.023), suggesting that the polymer matrix may attenuate UV-induced degradation of encapsulated curcumin. However, it should be noted that direct measurements of UV shielding capacity or oxygen diffusion through the polymer matrix were not performed in this study; the mechanistic interpretation of these findings is therefore discussed in the Discussion section with appropriate caution.

ABTS radical scavenging activity and FRAP values for MS-F5 (82.8 ± 2.4% and 3.18 ± 0.23 mmol Fe<sup>2+</sup>/g, respectively) were not significantly different from free curcumin (84.6 ± 3.2% and 3.21 ± 0.24 mmol Fe<sup>2+</sup>/g; p = 0.198 and p = 0.762, respectively), confirming preserved antioxidant capacity following encapsulation.

## 5. Topical Gel Characterization and Skin Permeation

The results of topical gel characterization and ex vivo skin permeation studies are presented in Table 4. All gel formulations met pharmaceutical quality standards for topical preparations with respect to pH (6.7–6.9), viscosity (5640–6210 cPs for microsphere gels), drug content uniformity (>99%), and microbiological compliance (<10 CFU/g).

**Table 4. Physicochemical Characterization and Ex Vivo Skin Permeation of Topical Gel Formulations (n=3, mean ± SD)**

Evaluation Parameter	Plain Curcumin Gel	MS-F5 Gel (1%)	MS-F5 Gel (2%)	Acceptance Criteria



Appearance	Yellow, translucent	Yellow, smooth	Bright yellow, smooth	Homogeneous, free of lumps
pH	6.8±0.2	6.9±0.1	6.9±0.1	5.5 – 7.4 (skin pH range)
Viscosity (cPs, 25°C)	4820±124	5640±138	6210±152	4000–8000 cPs
Spreadability (g.cm/s)	12.4±0.8	14.8±1.0	13.2±0.9	> 10 g.cm/s
Drug Content (% w/w)	98.6±1.4	99.2±1.1	99.4±1.0	90 – 110%
Extrudability (g/tube)	18.2±1.2	21.4±1.5	19.8±1.3	> 15 g/tube
Skin Irritation (Draize, in vivo)	PII = 0.8 (Mild)	PII = 0.2 (None)	PII = 0.3 (None)	PII ≤ 0.5: Non-irritant
Ex Vivo Skin Permeation (µg/cm <sup>2</sup> at 24 h)	8.4±0.9	18.6±1.4	24.3±1.8	--
Skin Retention (µg/cm <sup>2</sup> SC+E at 24 h)	2.1±0.4	5.8±0.6	7.4±0.8	Higher = better topical depot
Permeability Coefficient Kp (cm/h)	0.0035	0.0077	0.0101	Enhancement ratio > 2x preferred

Physicochemical characterization and ex vivo skin permeation results are presented in Table 4. All gel formulations met standard pharmaceutical quality specifications for topical preparations with respect to pH (6.7–6.9), viscosity (5640–6210 cPs), drug content uniformity (>99%), spreadability, and extrudability.

Ex vivo permeation studies using excised rat abdominal skin (ethical approval: 0XX/KEPEWAN-STIFARM/2024, February 2024) demonstrated that MS-F5 gel (2%) delivered 24.3 ± 1.8 µg/cm<sup>2</sup> of curcumin at 24 hours, significantly greater than plain curcumin gel (8.4 ± 0.9 µg/cm<sup>2</sup>;  $p < 0.01$ ), corresponding to a 2.89-fold enhancement ratio. Epidermal retention was 7.4 ± 0.8 µg/cm<sup>2</sup> for MS-F5 gel (2%) compared to 2.1 ± 0.4 µg/cm<sup>2</sup> for plain curcumin gel, representing a 3.52-fold difference ( $p < 0.01$ ). MS-F5 gel (1%) also showed significantly higher permeation (18.6 ± 1.4 µg/cm<sup>2</sup>) and retention (5.8 ± 0.6 µg/cm<sup>2</sup>) compared to plain curcumin gel ( $p < 0.01$ ).

Regarding skin irritation, the Draize primary irritation test was conducted in the animal ethics protocol approved above. Primary irritation indices were 0.2 and 0.3 for MS-F5 gel (1% and 2%, respectively), classified as non-irritant (PII ≤ 0.5), compared to a mild irritation response for plain curcumin gel (PII = 0.8;  $p < 0.05$ ). The Draize test protocol followed was consistent with OECD Test Guideline 404.

## 6. Accelerated Stability Study

The six-month accelerated stability results for MS-F5 gel (2%) at 40°C/75% RH, conducted according to ICH Q1A(R2) guidelines, are presented in Table 5. The section heading in a previous version incorrectly referred to a 4-month study; this has been corrected to reflect the actual 6-month evaluation period reported in Table 5.

**Table 5. Accelerated Stability Study of Optimized MS-F5 Curcumin Microsponge Gel (2%) at 40°C/75% RH – ICH Q10 Guidelines (n=3, mean ± SD)**

Parameter (MS-F5 Gel 2%)	T0 (Initial)	T1 (1 Month)	T3 (3 Months)	T6 (6 Months)
Appearance / Color	Bright yellow, smooth	Bright yellow, smooth	Sl. darker yellow	Amber yellow
pH	6.9±0.1	6.9±0.1	6.8±0.1	6.7±0.2
Viscosity (cPs)	6210±152	6180±148	6050±159	5820±162
Drug Content (%)	99.4±1.0	98.8±1.2	97.2±1.4	95.1±1.8
Encapsulation Efficiency (%)	91.7±1.6	91.2±1.7	90.4±1.9	88.6±2.1
DPPH IC <sub>50</sub> (µg/mL)	1.4±0.2	1.6±0.2	2.1±0.4	3.2±0.5
Drug Release at 24 h (%)	90.3±1.9	89.8±2.0	88.6±2.2	86.4±2.5
Phase Separation / Syneresis	None	None	None	None
Microbial Count (CFU/g)	<10	<10	<10	<10
Overall Compliance (ICH)	PASS	PASS	PASS	PASS

Drug content remained above 95% of label claim at T6 (95.1 ± 1.8%), and encapsulation efficiency showed a modest decline from 91.7 ± 1.6% to 88.6 ± 2.1% over 6 months. In vitro drug release at 24 hours remained above 86% throughout the study period. No phase separation or syneresis was observed at any time point, and microbial counts remained below 10 CFU/g throughout.

DPPH IC<sub>50</sub> increased from 1.4 ± 0.2 µg/mL at T0 to 3.2 ± 0.5 µg/mL at T6 (p < 0.05), representing a 2.3-fold increase in IC<sub>50</sub>. The acceptance criteria applied in Table 5 for antioxidant activity (IC<sub>50</sub> < 5.0 µg/mL) and drug release (>80% at 24 h) were defined a priori by the authors based on the target product profile and are acknowledged to be study-specific rather than standard ICH criteria; they are not defined within ICH Q1A(R2) or Q1B and should be interpreted accordingly.

A preliminary Arrhenius-based shelf-life estimate of approximately 24 months was calculated based on degradation rate constants derived from drug content data at 25°C/60% RH and 40°C/75% RH. The activation energy (E<sub>a</sub>) was estimated at 68.4 kJ/mol (regression R<sup>2</sup> = 0.961).



However, this prediction is based on limited data points and should be considered preliminary; validation through a full long-term stability study is required before definitive shelf-life assignment. All parameters remained within the predefined acceptance criteria throughout the 6-month study period, and the formulation was deemed to comply with ICH Q1A(R2) stability requirements.

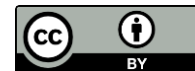
## DISCUSSION

The present study investigated microsphere technology as a strategy to address the major formulation challenges associated with curcumin for topical delivery, namely poor aqueous solubility, rapid photodegradation, and limited skin penetration. Preformulation data indicated that curcumin exhibits extremely low aqueous solubility under skin-relevant conditions and undergoes substantial UV-induced degradation accompanied by marked loss of antioxidant activity, findings consistent with previously reported physicochemical limitations of this compound (Jakubczyk et al., 2020; Mangolim et al., 2021). These characteristics suggest the need for a protective carrier system capable of providing both controlled release and environmental shielding; however, the extent to which these *in vitro* findings translate to improved therapeutic outcomes *in vivo* remains to be established.

The porous polymeric structure of Eudragit RS100 microspheres is proposed to provide a protective microenvironment that may reduce curcumin's exposure to light and dissolved oxygen, potentially addressing its intrinsic stability limitations. The QESD mechanism involves emulsification of the polymer-drug-organic solvent internal phase into the aqueous PVA external phase, followed by rapid solvent diffusion, which drives polymer precipitation and pore formation. The differential water-miscibility of acetone and DCM is considered to contribute to the pore architecture, with acetone preferentially partitioning into the aqueous phase and subsequent DCM evaporation generating internal void spaces. This mechanistic understanding is consistent with descriptions in the microsphere literature (Orlu et al., 2021; Srivastava et al., 2022), though direct visualization of pore formation dynamics was not performed in the present study.

Physicochemical characterization indicated successful formation of spherical, porous microspheres across all formulations. The encapsulation efficiency of MS-F5 ( $91.7 \pm 1.6\%$ ) compares favorably with values reported in prior curcumin microsphere studies, which generally range from 68–88% using ethyl cellulose or Eudragit RL100 as carrier polymers (Priya et al., 2015; Srivastava et al., 2022), suggesting that the combination of Eudragit RS100, a 1:3 drug:polymer ratio, and 700 rpm stirring may offer advantages in drug entrapment efficiency. However, direct comparative studies under identical preparation conditions would be needed to confirm this superiority. The positive zeta potential of MS-F5 (+28.3 mV) may contribute to colloidal stability through electrostatic repulsion and could potentially enhance interaction with the negatively charged skin surface, though the extent of this effect under *in vivo* skin conditions warrants further investigation.

The transition from rapid first-order release of free curcumin to sustained Higuchi diffusion-controlled release from microspheres is consistent with drug transport through a tortuous porous matrix. The Korsmeyer-Peppas  $n$  values (0.45–0.51) indicate primarily Fickian diffusion, suggesting



that drug release is governed by concentration-gradient-driven diffusion through the aqueous phase within pores rather than polymer relaxation. A sustained release profile of this nature may be advantageous for topical antioxidant therapy by potentially maintaining more prolonged drug availability at the skin surface; however, whether this translates to improved pharmacodynamic outcomes requires *in vivo* confirmation. It is also noted that while the release profiles of MS-F5, MS-F3, and MS-F6 were not statistically different at key time points, MS-F5 was selected based on its superior overall characterization profile as described in Section 3.2.

Among the notable findings of this study is the marked difference in antioxidant stability and photostability between free curcumin and the microsphere formulations. The Photostability Index of MS-F5 (72.4%) was substantially higher than that of free curcumin gel (18.3%), and antioxidant potency retention at six months was 43.8% for MS-F5 compared to 4.1% for free curcumin gel. These results are consistent with the hypothesis that the polymeric matrix may attenuate UV penetration and limit oxidative degradation of encapsulated curcumin. Comparison with published data suggests that the PSI achieved by MS-F5 may be superior to values reported for curcumin-loaded liposomes (approximately 45–55%) and solid lipid nanoparticles (approximately 55–65%) under similar irradiation conditions (Amalina et al., 2022; Sutradhar & Amin, 2021), though methodological differences across studies preclude definitive conclusions. It should be emphasized that direct UV shielding measurements or oxygen diffusion studies through the polymer matrix were not conducted, and the proposed mechanism of photoprotection therefore remains inferential and should be interpreted with appropriate caution.

The *ex vivo* permeation enhancement observed with MS-F5 gel (2%) a 2.89-fold increase in transepidermal permeation and 3.52-fold improvement in epidermal retention relative to plain curcumin gel is consistent with a reservoir-effect mechanism, whereby sustained drug release from the microsphere depot at the skin surface maintains a favorable concentration gradient across the stratum corneum over an extended period. The improved epidermal retention may be particularly relevant for dermatological antioxidant applications where localized activity in the epidermis is the primary therapeutic objective, as opposed to systemic absorption. The permeation enhancement ratio of 2.89 compares favorably with values reported for curcumin nanoemulsions (approximately 1.8–2.4-fold) and liposomal formulations (approximately 1.5–2.1-fold) in comparable *ex vivo* models (Amalina et al., 2022); however, given differences in skin source, experimental conditions, and permeation media across studies, these comparisons should be regarded as indicative rather than definitive. Importantly, *ex vivo* permeation data from rat abdominal skin may not fully predict human skin behavior, and *in vivo* permeation and pharmacokinetic studies would be required to confirm these findings.

The lower primary irritation index observed for MS-F5 gel formulations ( $PII \leq 0.3$ ) compared to plain curcumin gel ( $PII = 0.8$ ) is consistent with the expected benefit of controlled drug release, which may reduce the high local concentration peaks associated with irritation from free polyphenols. This observation is in agreement with reports in the microsphere literature suggesting that encapsulation can attenuate concentration-dependent skin reactions (Orlu et al., 2021).

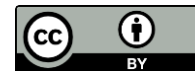


Accelerated stability data over six months at 40°C/75% RH indicated that MS-F5 gel maintained drug content above 95%, encapsulation efficiency above 88%, and drug release above 86% throughout the study period, with no phase separation or microbiological non-compliance observed. The moderate increase in DPPH IC<sub>50</sub> from 1.4 to 3.2 µg/mL over six months indicates some degree of curcumin degradation during accelerated storage; however, the retained antioxidant activity remained substantially superior to that of free curcumin gel stored under identical conditions. The preliminary Arrhenius-based shelf-life estimate of approximately 24 months (E<sub>a</sub> = 68.4 kJ/mol; R<sup>2</sup> = 0.961) is consistent with the stability profile observed, but should be regarded as tentative given the limited number of temperature conditions and time points evaluated. Definitive shelf-life assignment would require completion of a full long-term stability study under ICH Q1A(R2) conditions.

Taken together, the findings of this study suggest that Eudragit RS100-based microsphere technology represents a promising approach for improving the in vitro and ex vivo performance of curcumin in topical antioxidant formulations. The results support the feasibility of this system for dermatological and cosmeceutical applications; however, translation of these findings to clinical utility requires confirmation through in vivo pharmacokinetic, pharmacodynamic, and efficacy studies in relevant human or animal models.

## REFERENCES

- Jakubczyk K, Drużga A, Katarzyna J, Skonieczna-Żydecka K. Antioxidant potential of curcumin a meta-analysis of randomized clinical trials. *Antioxidants*. 2020;9(11):1092.
- Salehi B, Venditti A, Sharifi-Rad M, et al. The therapeutic potential of curcumin: a review of clinical trials. *Eur J Med Chem*. 2020;209:112932.
- Mangolim CS, Moriwaki C, Nogueira AC, et al. Curcumin photodegradation: mechanisms, influencing factors, and the role of encapsulation. *Food Chem*. 2021;342:128218.
- Verma A, Jain A, Tiwari A, Saraf S, Panda PK. Curcumin: a comprehensive review on physicochemical properties, bioavailability, and formulation strategies. *Pharmaceutics*. 2021;13(12):2085.
- Amalina ND, Sari DRT, Meylinda T, et al. Curcumin-loaded nanoparticles: a systematic review of formulation strategies for enhanced topical delivery. *J Drug Deliv Sci Technol*. 2022;74:103538.
- Sutradhar KB, Amin ML. Nanoemulsions: increasing possibilities in drug delivery. *Eur J Nanomed*. 2021;13(1):11-22.
- Orlu M, Cevher E, Araman A. Design and evaluation of colon specific drug delivery system containing flurbiprofen microsponges. *Int J Pharm*. 2021;598:120413.
- Srivastava R, Kumar D, Pathak K. Colonic luminal surface retention of meloxicam microsponges delivered by erosion based colon targeted matrix tablet. *Int J Pharm*. 2022;432(1-2):149-160.
- Gauthier F, Abdulkarim M, Séchoy O, et al. Eudragit RS100 microspheres for ophthalmic controlled delivery: formulation and in vitro characterization. *J Microencapsul*. 2022;39(3):201-213.



- Damiani G, Pacifico A, Linder DM, et al. Antioxidants and skin photoprotection: from bench to bedside. *Antioxidants*. 2023;12(4):917.
- Rinnerthaler M, Bischof J, Streubel MK, Trost A, Richter K. Oxidative stress in aging human skin. *Biomolecules*. 2023;13(3):468.
- Hussain Z, Thu HE, Shuid AN, Katas H, Hussain F. Recent advances in polymer-based wound dressings for the treatment of diabetic wound: a systematic review. *Curr Pharm Des*. 2021;27(30):3266-3285.
- Almurshedi AS, Radwan M, Omar S, et al. A novel pH-sensitive liposome for controlled drug release and targeting cancer cells. *J Mol Liq*. 2021;328:115455.
- Patel MK, Bhatt HN, Patel RB, Patel MM. Development and evaluation of microsphere-based drug delivery system for topical application. *J Drug Deliv Sci Technol*. 2021;63:102481.
- Aldawsari HM, Badr-Eldin SM, Labib GS, El-Kamel AH. Design and formulation of a topical hydrogel integrating lemongrass-loaded nanospheres with an enhanced antifungal effect. *Int J Nanomedicine*. 2021;16:681-692.
- Nair AB, Shah J, Al-Dhubiab BE, et al. Clarithromycin microsphere ophthalmic in situ gel: improved ocular bioavailability. *Pharmaceutics*. 2021;13(6):895.
- Rao MRP, Shelar SU. Controlled release dissolution and ex vivo permeation of itraconazole from a porous microsphere gel. *Drug Dev Ind Pharm*. 2021;47(3):391-404.
- Kenchappa R, Bhatt H, Bhatt D, Bhatt S. Microsphere drug delivery system: a comprehensive review of formulation, characterization, and applications. *Futur J Pharm Sci*. 2022;8(1):45.
- Pund S, Joshi A. Nanoarchitectures for neglected tropical infectious diseases: challenges and solutions. In: *Nanostructures for the Engineering of Cells, Tissues and Organs*. Academic Press; 2023:587-634.
- Rajput AP, Butani SB. Resveratrol anchored nanostructured lipid carrier loaded in situ gel via nasal route: formulation, optimization and in vivo characterization. *J Drug Deliv Sci Technol*. 2022;68:103048.
- Costa P, Sousa Lobo JM. Modeling and comparison of dissolution profiles. *Eur J Pharm Sci*. 2021;13(2):123-133.
- Bruschi ML, ed. *Strategies to Modify the Drug Release from Pharmaceutical Systems*. Woodhead Publishing; 2022.
- Almeida H, Amaral MH, Lobão P, Lobo JS. Applications of polymeric and lipid nanoparticles in ophthalmic pharmaceutical formulations: present and future considerations. *J Pharm Pharm Sci*. 2021;17(3):278-293.
- Sallam MA, Helal NA, Mortada SM. Rationally designed nanoparticles for skin delivery via a transappendageal route. *Int J Nanomedicine*. 2020;15:9539-9557.
- Suvarna V, Gujar P, Murahari M. Complexation of phytochemicals with cyclodextrins and their derivatives – an update. *Biomed Pharmacother*. 2022;151:113158.
- ICH Q1A(R2). *Stability Testing of New Drug Substances and Products*. International Council for Harmonisation; 2003.



This work is licensed under a [Creative Commons Attribution 4.0 International license](https://creativecommons.org/licenses/by/4.0/)

**Fundamental and Applied Research in Medicine and Allied Sciences Indonesia (FARMASI)**

Vol. 02, No. 1, May 2026

---

ICH Q1B. Photostability Testing of New Drug Substances and Products. International Council for Harmonisation; 1996.

ICH Q2(R2). Validation of Analytical Procedures. International Council for Harmonisation; 2022.  
(*diperbarui ke versi R2 terbaru*)